Journal of Mammalian Evolution (2023) 30:1031–1046
https://doi.org/10.1007/s10914-023-09688-y

RESEARCH

Rib remodelling changes with body size in fossil hippopotamuses from Cyprus and Greece

Justyna J. Miszkiewicz[1,2] · Athanassios Athanassiou[3] · George A. Lyras[4] · Alexandra A. E. van der Geer[1]

Accepted: 28 September 2023 / Published online: 3 November 2023

Abstract

Large species that are isolated for thousands of years on islands often evolve extreme degrees of dwarfism. Very little is known about physiological processes that accompany such extreme transitions in extinct dwarf species. We tested whether physiological cycles of bone maintenance (remodelling) in dwarf adult hippopotamuses correlate with insularity-driven body mass shifts that may occur due to variables such as ecological release from predation pressure and change in access to resources. We hypothesised that hippopotamuses with the smallest body size should show higher values of osteocyte lacunae, proxies for osteoblast proliferation during cycles of remodelling, when compared to relatively larger dwarf forms, as well as much larger mainland common hippopotamuses. We examined 20 ribs from three extinct Pleistocene *Hippopotamus* species spanning a gradient in body size: *H. minor* (~132 kg, Cyprus), *H. creutzburgi* (~398 kg, Crete), and *H. antiquus* (~3200 kg, mainland Greece). Ribs were selected because they reflect bone metabolic rates that are not completely clouded by factors such as biomechanics. Densities of osteocyte lacunae (Ot.Dn) were examined in 864 individual secondary osteons observed in histology sections. We found the highest average Ot.Dn in the *H. minor* ribs, intermediate Ot.Dn in the *H. creutzburgi* ribs, and the lowest Ot.Dn in the *H. antiquus* ribs. It appears that Ot.Dn distinctly separated these three species, possibly signifying a gradient in bone remodelling such that bone tissue optimises maintenance in the face of insularity-driven reduction of body size. We discuss hippopotamus rib bone microstructure and the utility of Ot.Dn in palaeontological analyses for elucidating intricate biological processes occurring in bone of insular fossil mammals.

Keywords Fossil mammals · Haversian bone · *Hippopotamus* · Insularity · Palaeohistology

Introduction

Mammals on islands can evolve into dwarfs or giants in response to changes in extrinsic variables such as ecologically relevant competition and predation, resource availability, evolutionary time in isolation, climate and according to intrinsic variables such as bauplan, ancestral body mass and dietary adaptations (Lomolino et al. 2013; Benítez-López et al. 2021; van der Geer et al. 2021). This poses a threat to the metabolic-life history balance as body size undergoes change, and mammals may modify their life history traits to ensure viable reproduction (Köhler et al. 2010). As a result, a typically "slow growing" mammal in life history terms might undergo an acceleration in some physiological aspects to adapt to body size changes moving towards selected "fast" life history traits (Raia et al. 2003; Sibly and Brown 2007; Köhler et al. 2010). Most of our current knowledge about body mass variation in extinct insular and mainland mammals stems from gross anatomical observations in

✉ Justyna J. Miszkiewicz
justyna.miszkiewicz@naturalis.nl

✉ Alexandra A. E. van der Geer
alexandra.vandergeer@naturalis.nl

[1] Vertebrate Evolution, Development and Ecology, Naturalis Biodiversity Center, Leiden 2333, The Netherlands

[2] School of Social Science, University of Queensland, Brisbane 4072, Australia

[3] Ministry of Culture, Ephorate of Palaeoanthropology and Speleology, Arditou, Athens 11636, Greece

[4] Department of Geology and Geoenvironment, National and Kapodistrian University of Athens, Panepistimiopolis, Athens 15784, Greece

extant and extinct taxa (Raia and Meiri 2006; Lomolino et al. 2013; van der Geer et al. 2021). Among extinct mammal taxa, there are some extraordinary examples of insular body size shifts such as small-sized elephants (e.g., *Palaeoloxodon falconeri*, *Palaeoloxodon cypriotes*, *Stegodon sondaari*; van der Geer et al. 2006) and large-sized mice (e.g., *Canariomys bravoi*, *Coryphomys buehleri,* and *Leithia melitensis*; Michaux et al. 1996; van den Hoek Ostende et al. 2014). Fossil evidence for body mass evolution can offer an insight into the extremes of body mass plasticity under island conditions that cannot be gleaned from living animal observations alone. Further, in well-preserved fossil specimens, where their bone microstructure is not obliterated by taphonomic agents, it has been possible to access biological data beyond gross skeletal observation and infer life history traits from bone microstructure (histology) organisation which reflects ontogenetic tissue growth, and physiological bone processes during lifespan in later stages (e.g., Köhler and Moyà-Solà 2009; Kolb et al. 2015; Orlandi-Oliveras et al. 2018; Miszkiewicz et al. 2019, 2020; Miszkiewicz and van der Geer 2022). These physiological processes refer to a cyclical pattern of bone tissue renewal that occurs throughout the lifespan and ensures blood supply to bone, maintenance of the calcium reservoir, bone structural integrity and damage repair (Hart et al. 2020). Remodelling can be influenced by intrinsic biological and extrinsic environmental cues (Robling et al. 2006). Compared to gross anatomical approaches, there have been fewer of such histology studies within palaeontology, but owing to their technical capacity to reach cell-level information, new hypotheses about how insular animals adjust their physiology in the face of insularity have emerged. While most histology applied to dwarf or giant mammals has focussed on bone micro-architecture relating to ontogeny, a handful of studies targeting bone renewal processes (remodelling), and bone maintenance at the cell (osteocyte) level, has identified a possible link, or gradient, between body size evolution due to dwarfism or gigantism and physiological cycles of bone tissue maintenance in fossil murines (Miszkiewicz et al. 2020), deer (Miszkiewicz and van der Geer 2022), and extant hippopotamuses (Bromage et al. 2009). Building on this research, we here test for this link in dwarf and mainland extinct hippopotamuses from Pleistocene Greece and Cyprus to further investigate whether the body size-osteocyte lacunae relationship holds in these fossil species.

(Palaeo)histology of insular mammals

As vertebrates develop during ontogeny, the bone tissue constituting their skeleton changes in micro-anatomy such that speed of formation show corresponding bone organisation (lamellar, parallel-fibred, fibrolamellar, or woven-fibred bone) with varying micro-morphologies of vascularity (orientation and connectedness) (Francillon-Vieillot et al. 1990). This premise, in combination with gross skeletal measurements and palaeontological context, is used by (palaeo) histologists to assess traits such as animal growth or maturation stages, and thus aspects of longevity, but also aspects of ecology or environmental factors, such as insularity (Padian and Lamm 2013; Kolb et al. 2015; Whitney et al. 2022). A review by Kolb et al. (2015) focussing on cynodonts and mammals described reticular and plexiform fibrolamellar bone in juvenile dwarf *Hippopotamus minor*; parallel-fibred primary bone, reticular vascularity, and Haversian bone in giant *Mikrotia magna;* lamellar and compact coarse cancellous bone in giant *Leithia* sp.; parallel-fibred primary bone, and complex (reticular, radial, and longitudinal) vascularity in giant *Prolagus;* and Haversian bone in a giant *Paraceratherium*. Kolb et al. (2015) indicated that such a range of bone histologies within each taxon reflects modifications in growth rates in response to insular conditions, and relates to factors such as biomechanics, island geography, climate, and timeline of dwarfism/gigantism evolution. Miszkiewicz et al. (2019) observed highly developed Haversian bone in the femur of a giant murid from Timor, linking it to favourable environments, such as lessened predation and higher resource availability, occurring in the late Holocene in that region which might have facilitated rat longevity and body size expansion allowing for bone to accumulate osteons. More recently, we observed advanced Haversian bone formation in the ribs of dwarf *Candiacervus* from Pleistocene Crete, likely indicating extended longevity unexpected for the dwarf body size (Miszkiewicz and van der Geer 2022).

The above bone histology associations with evolution on islands offer a promising avenue from which to test further hypotheses about cell-level maintenance of bone tissue along body mass shifts. Work considering dwarfs/giants, or species of different body masses, at the osteocyte-level has so far considered cortical bone in fossil murine femora, including giants, from Timor (Miszkiewicz et al. 2020); trabecular bone in the proximal part of femora of extant rats, rabbits, Rhesus monkeys, pigs, and cows (Mullender et al. 1996); and periosteal lamellar bone in extant and extinct primates (catarrhines and strepsirrhines), and selected pygmy and common mammals (*Rattus* and *Hippopotamus*) (Bromage et al. 2009). In all these instances, an inverse relationship between body mass and osteocyte/ lacunae (osteocyte cells reside within microscopic lacunae in fossil specimens where cells themselves do not survive post-mortem, Fig. 1) densities was found, suggesting that higher body mass is affiliated with slower bone remodelling, possibly due to proportionate differences in basal metabolic outputs. A larger, cross-mammalian study of bone histology by Felder et al. (2017) (not addressing insular mammals) reported negative allometry in secondary osteon area with body mass in stylopod bones, which was not linked with phylogeny. As

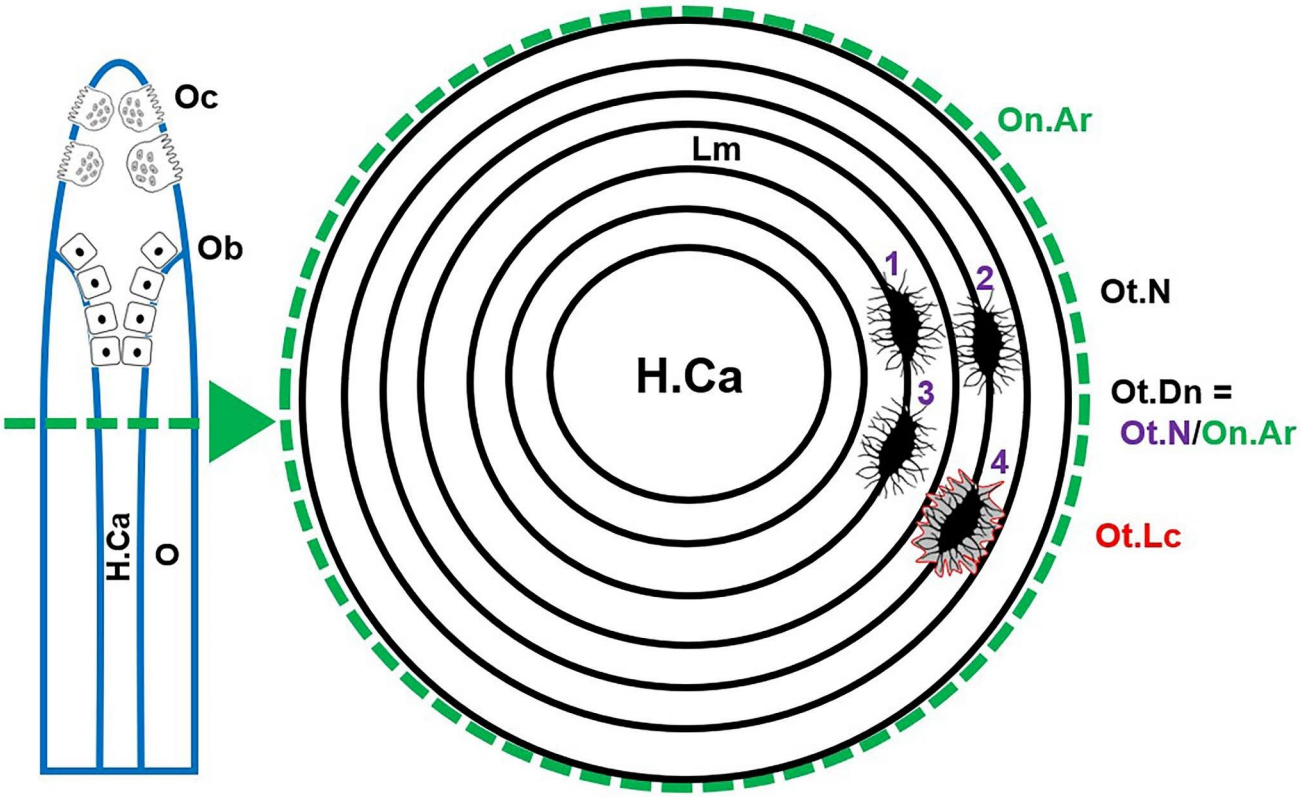

Fig. 1 Schematic diagram illustrating secondary osteon histology variables examined in the present study (**On.Ar**: secondary osteon area; **Ot.Dn**: secondary osteon lacuna density). The blue "cone" to the left of the diagram illustrates an active bone multicellular unit with osteoclasts (**Oc**) resorbing bone, osteoblasts (**Ob**) depositing new unmineralised bone (**o**: osteoid), surrounding a Haversian canal (**H.Ca**) that is about to be formed. Osteocyte lacunae (**Ot.Lc**), cavities housing osteocytes (**Ot**), were counted from across lamellae (**Lm**) formed in each secondary osteon. Abbreviations follow bone histomorphometry nomenclature standards by Dempster et al. (2013)

secondary osteons form through the bone multicellular unit (BMU) activity, where osteoclasts and osteoblasts resorb and form bone respectively (Fig. 1), Felder et al. (2017) indicated that bone resorption area in small mammals could be constrained to mitigate fracture risk but maintain osteocyte function in larger mammals. However, whether secondary osteons and matched osteocytes within, as direct products of bone remodelling (in Haversian bone) (Currey et al. 2017), undergo similar changes under insular body mass conditions, is currently unknown. Our paper addresses this gap of knowledge by focusing on three closely related fossil species of hippopotamuses.

Extinct and extant hippopotamus bone histology

Throughout their evolutionary history, hippopotamuses showed a wide range of body size variation ranging from just over 100 kg to well above 3 tonnes (van der Geer et al. 2021). Hippopotamuses are semi-aquatic animals that have relatively short legs and dense bones of high mass with graviportal anatomical adaptations so their whole body can sink down and charge submerged through the water (Houssaye et al. 2021). Several insular dwarf hippopotamuses have been described, including *Hippopotamus lemerlei* and *H. madagascariensis* from Late Pleistocene-Holocene Madagascar (Grandidier in Milne Edwards 1868; Stuenes 1989), and those that evolved during the Pleistocene on larger Mediterranean islands such as *H. creutzburgi* from Crete (Boekschoten and Sondaar 1966), *H. minor* from Cyprus (Boekschoten and Sondaar 1972; named therein as *Phanourios minor*), *H. melitensis* from Malta (Major 1902), and *H. pentlandi* from Sicily (von Meyer 1832). Species larger than the common, extant *H. amphibius* included the "European hippopotamus" *H. antiquus* (Deraniyagala 1955; Faure 1981) and *H. gorgops* (Dietrich 1928; Martinez-Navarro et al. 2022). Today, Hippopotamidae are represented by two genera and species, *H. amphibius* and *Choeropsis liberiensis*, both native to Africa, of which the latter is a pygmy form (Fröhlich et al. 2017).

We have limited knowledge regarding bone histology of extinct and extant hippopotamuses (e.g., Gray et al. 2007; Kolb et al. 2015; Cooper et al. 2016). Kolb et al. (2015) reported reticular to plexiform fibrolamellar bone formation in the femora and tibiae of small to large juvenile specimens of the dwarf *H. minor* of Cyprus, which was interpreted as matching bone growth patterns in continental artiodactyls.

Gray et al. (2007) sectioned a mid-thoracic rib of *C. liberiensis* with an initial aim to examine bone compactness, but the rib appeared pathological with widespread osteoarthritic growths, abnormally thin cortical bone and high porosity, yielding no usable data. Using high-resolution micro-computed tomography (micro-CT), Cooper et al. (2016) noted thickening of cortical bone of the humerus, femur, and tibia in *H. amphibius*. Bone shape and structure in *C. liberiensis* and *H. amphibius* was previously inferred to reflect adaptation to semi-aquatic lifestyles from cortical bone thickening and spongiosa occurring in the medullary cavity (Hayashi et al. 2013; Houssaye et al. 2016a, b; 2021).

Research question

In our recent study of the dwarf *Candiacervus* (Miszkiewicz and van der Geer 2022), we found the rib tissue to show advanced Haversian bone with multiple generations of secondary osteons which we would expect to see in large and long-living mammals. However, a limitation of our study was a lack of a mainland/ ancestor species to compare the results to. Further, we were not able to examine cell-level data regarding bone remodelling cycles due to inconsistent microstructure preservation which obliterated osteocyte lacunae. Ribs are increasingly recognised as useful bones for addressing remodelling questions in various mammals, including humans (Pitfield et al. 2019; Stewart et al. 2021) and elephants (Basilia et al. 2023a, b). Studies have suggested that due to its less biomechanically stimulated environment than that of limb bones, ribs should reflect less variable cyclical remodelling reflecting physiological needs for calcium homeostasis and bone quality maintenance rather than experiencing frequent remodelling targeting biomechanically damaged bone regions (see review and discussion in Stewart et al. 2021). Stewart et al. (2021) tested and confirmed this using a kangaroo (as a hopping mammal model experiencing a range of mechanical loads on its skeleton) whose ribs, compared to long bones, showed higher bone vascularity facilitating increased blood supply. Building upon the osteocyte and body mass studies outlined earlier, and our recent attempt to examine Haversian bone remodelling in the ribs of insular deer, we hypothesised that hippopotamuses on the lower end of dwarfism spectrum (i.e., relatively smaller body size) should show evidence of higher bone remodelling (i.e., higher counts of osteocyte lacunae) when compared to relatively larger dwarf forms, as well as much larger mainland common hippopotamuses.

Table 1 List of rib specimens examined in the present study

Locality	Species	Specimen ID	Rib identification
Cyprus, Akanthou (CAK) and Ayia Irini	*Hippopotamus minor*	Akanthou CAK	Midshaft
		Akanthou CAK 2	Proximal shaft, left?
		Akanthou CAK 3	Proximal shaft, left?
		Ayia Irini II R1	Proximal shaft
		Ayia Irini II R2	Midshaft
		Ayia Irini II R3	Midshaft
		Ayia Irini II R4	Midshaft
		Ayia Irini II R5	Distal shaft
Crete, Katharo Basin	*Hippopotamus creutzburgi*	KA-Σ-35	Midshaft
		KA-Σ-59	Midshaft
		KA-Σ-96	Midshaft
		KA-Σ-97	Midshaft
		KA-Σ-98	Midshaft
		KA-Σ-101	Midshaft
		KA-Σ-193	Midshaft
Mainland Greece, Peloponnesos, Megalopolis Basin	*Hippopotamus antiquus*	P1	Unidentifiable piece of shaft
		P2	Unidentifiable piece of shaft
		P3	Unidentifiable piece of shaft
		P4	Unidentifiable piece of shaft
		P5	Unidentifiable piece of shaft

Materials and methods

Fossil rib specimens

A total of 20 rib fragments from adult hippopotamus fossils were examined in our study. Eight ribs were from *H. minor*, seven belonged to *H. creutzburgi*, and five were from *H. antiquus*. All of the specimens derive from localities spanning Pleistocene Greece and Cyprus (Table 1; Fig. 2), and the three species were selected as they reflect a clear progression in body size evolution with the smallest *H. minor* (~132 kg, Akanthou and Ayia Irini II localities in Cyprus), "slightly" larger *H. creutzburgi* (~398 kg, Katharo Basin locality in Crete), and the largest *H. antiquus* (~3200 kg, Megalopolis Basin in Peloponnesos, mainland Greece; body mass from Lomolino et al. 2013). *H. minor* (also known as *Phanourios minor*; but see genomic analysis by Psonis et al. 2021) occurred in Cyprus during the Late Pleistocene and is the smallest dwarf hippopotamus to have ever existed. The dwarf *H. creutzburgi* is thought to have walked on its hooves due to occurrence in a rocky rather than mostly aquatic environment. Compared to its mainland counterpart (and the most likely ancestral species, but not necessarily ancestral population), *H. antiquus*, *H. creutzburgi* had a longer humerus, but a shorter radius, along with shorter feet bones, which reflects some changes in body proportions in the dwarf (Spaan 1996; van der Geer et al. 2021). Unlike hippopotamuses today, both *H. minor* and *H. creutzburgi*

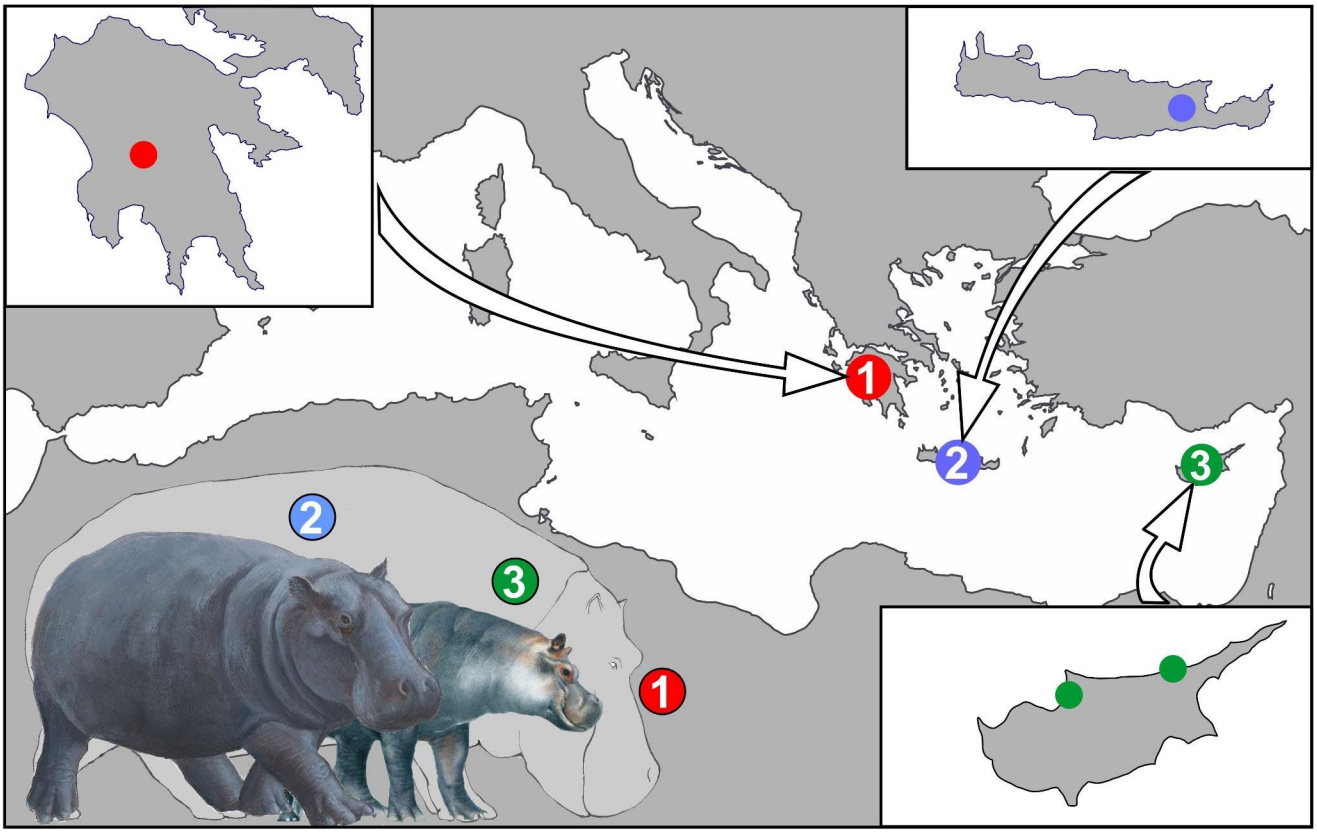

Fig. 2 Map of the Mediterranean Region showing palaeontological localities (circles in inset boxes) and reconstructions of hippopotamus species examined in our study. **a**. The Peloponnese Peninsula with the site Megalopolis Basin, which has yielded *Hippopotamus antiquus*; **b.** the Island of Crete with the site Katharo Plain, which has yielded *H. creutzburgi*; **c**. the island Cyprus with the sites Akanthou (east) and Ayia Irini (west), which has produced remains *H. minor*. Images and maps courtesy of George Lyras

are thought to have occupied rugged terrain rather than lowlands near rivers and lakes to support their mostly semi-aquatic lifestyles (van der Geer et al. 2021; Georgitsis et al. 2022). *H. antiquus* was a large hippopotamus (larger than extant *H. amphibius*) occurring during the Middle Pleistocene in Europe (Martino and Pandolfi 2022), and its lineage originated in Africa (Mazza 1991). However, *H. antiquus* is thought to have relied more on aquatic environments than *H. amphibius*, at least at localities in England (Adams et al. 2022).

Ribs were identified from fossil commingled, multi-individual assemblages of disarticulated hippopotamus material and selected on the basis of preservation of the shaft portion of each rib. We were able to confidently identify the fragments as ribs because they all had rib characteristics preserved (Online Resource 1). For example, some had the tubercle and head portion preserved along with the diagnostic curvature forming the vertebral end, all had a clear costal groove, and some pieces showed clear flatness characteristic of the sternal end (Online Resource 1). The exact anatomical identification (i.e., rib number in the rib cage) of each rib was not possible given their fragmentation, but it was possible to determine the side and distance from the proximal/distal ends of each rib (Table 1). We had aimed for the entirety of rib shaft cross-section (in a transverse plane) to be preserved so that we could examine bone histology across the walls of the cortical bone along with the morphology of the medullary cavity. This was possible in all specimens of *H. minor* and *H. creutzburgi*, but not in *H. antiquus*. The *H. antiquus* ribs were in fragmented pieces (Online Resource 1). A limitation in our study is that we cannot ascertain if the *H. antiquus* pieces derive from the same rib and individual and whether the *H. minor* and *H. creutzburgi* rib fragments represent different individuals. On the basis of gross preservation (colour and morphological characteristics; see Online Resource 1), we can hypothesise that each rib was indeed from a different individual in at least *H. minor* and *H. creutzburgi*.

Section extraction and histology slide preparation

Each rib fragment was documented pictorially and a sectioning location was marked with a pencil (Online Resource 1). The diameter of ribs (Rib.dm) in an inferior-superior plane

was measured three times using digital callipers (Mitutoyo). The sections removed for histology were approximately 1–1.5 cm thick. The ribs were processed for histology in two different laboratory facilities (Histology lab at the Australian National University in Canberra, and GeoLab at Naturalis Biodiversity Center in Leiden) due to COVID-19 restrictions, but following the same protocol and prepared by the same histologist (Miszkiewicz), following methods reported in Miszkiewicz and van der Geer (2022) and Walker et al. (2020). The sections were removed using a Dremel drill equipped with a carbide cutting blade. Holding the spinning blade perpendicular at a right angle to the bone surface, two parallel cuts were made into the bone exterior moving deeper into the bone until a complete cut was made through the rib shaft.

To produce thin sections, we followed standard histology techniques as reported in fossil rib histology studies (e.g., Stewart et al. 2021; Miszkiewicz and van der Geer 2022). Each section was embedded in epoxy resin (Buehler EpoxyCure and Huntsman Araldite), and cut in a transverse plane through the rib shaft using a diamond wafering blade on a low-speed saw (Kemet MICRACUT 1000 and Struers Accutom-2). The revealed histology surface was gently polished on a fine grinding pad (1200 grit) to remove scratches, dried, and mounted on microscope glass slides using Araldite epoxy glue. Each mounted slide was then attached to a dedicated saw vise for slides so that the remaining portion of the section could be trimmed down to 300–500 µm thickness. The slides were then reduced to an approximate thickness of 100 µm (+/- 10 µm) on a series of grinding pads (ranging from 400 to 1200 grit size) and polished using a Buhler diamond polishing powder paste. At this stage, each slide was examined under a basic optical microscope to confirm suitable preservation for further analyses. Each slide was then cleared in an ultrasonic cleaner, dehydrated in a series of ethanol baths starting at 75% and ending in absolute ethanol, and cleared with xylene. A cover slip was then placed on each slide using a DPX mounting medium.

Histology imaging and image analysis

First, we assessed the thin sections for bone types by examining overall thin sections under a series of magnifications (4x–20x) using Olympus BX53, BX60 and Nikon Eclipse

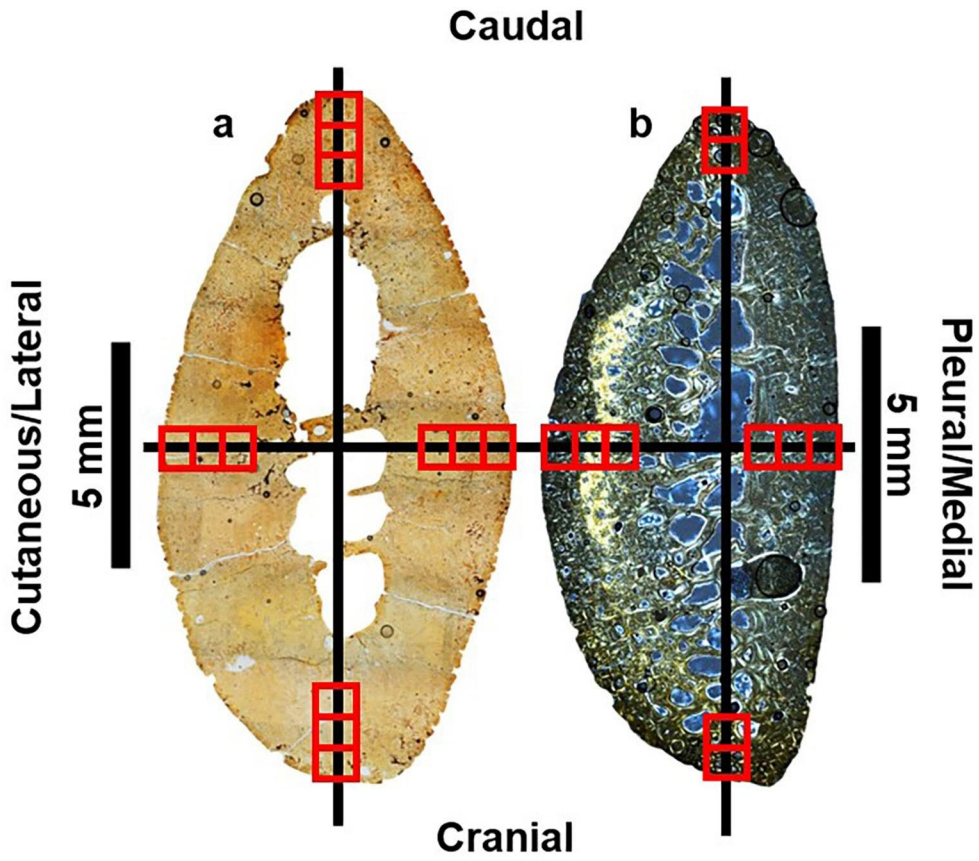

Fig. 3 Diagram illustrating the region of interest (ROI) selection procedure. **a**. *H. minor* Ariya Irini II R4 specimen under transmitted light; **b**. *H. minor* CAK specimen under polarised light. Crosses reflecting x and y axes determine the collection of images starting at the mid-point of the periosteal border on each anatomical aspect (pleural, cutaneous, caudal, cranial). Some cortical walls were too thin to capture three ROIs as can be seen in b. The ROI red rectangles are not to scale

E600 POL microscopes. Our observations were based on qualitative bone tissue characteristics as defined by Francillon-Vieillot et al. (1990), focusing on vascularity (orientation and type), collagen fibre orientation, bone tissue types (primary/secondary), and morphological features of osteons (shape, size, clustering). All sections showed well-remodelled Haversian bone which we needed to conduct further high-resolution examination at the secondary osteon and osteocyte lacuna-level. We worked with individual secondary osteons because each one reflects a single BMU event (Chang and Liu 2022).

Second, we applied a region of interest (ROI) approach to all slides to ensure that we capture secondary osteon data from consistent rib locations. The rib cross-section was orientated with the rib cranial and caudal aspects forming y and x axes respectively (Fig. 3). Three successive ROIs placed along y and x axes super-imposed over each slide (Fig. 3) were captured from the caudal, cranial, pleural, and cutaneous anatomical regions at a magnification of 10x using digital microscope cameras (Olympus DP74; MIchrome 5 Pro SS-936 camera; Nikon D-Ri2). We took representative images of complete slides using the auto-stitching function in Olympus CellSens software, and by manual stitching of overlapping images in Photoshop. The first ROI was always located at the mid-point of the outermost edge of the periosteal border allowing for placement of the subsequent ROIs moving away from the first ROI into the deep cortex. In almost all slides it was possible to collect three ROI images, but there were instances where cortical walls were thin enough to only fit two ROIs.

Histology images were then individually inspected for preservation of intact secondary osteons showing clear cement lines and completed formation where a Haversian canal can be clearly seen, rather than a, for example, half-filled secondary osteons or just resorption cavities. This way, we were able to select secondary osteons that had completed formation before each animal's death, and they reflect a complete cycle of the different osteon remodelling stages: activation, resorption, and formation (Frost 2001). Their "unremodelled condition" (lack of partial resorption by successive secondary osteons) means we can infer for these units to be younger than those that had formed in older (earlier) remodelling cycles. From within each image, all well-preserved osteons were marked and manually extracted in Fiji/ImageJ using the "Freehand selection" and "Crop" tools. Individual secondary osteon images had a scale bar burnt in and were saved as separate files, resulting in a total of 864 individual secondary osteons (383 in *H. minor*, 381 in *H. creutzburgi*, and 100 in *H. antiquus*) (Fig. 4).

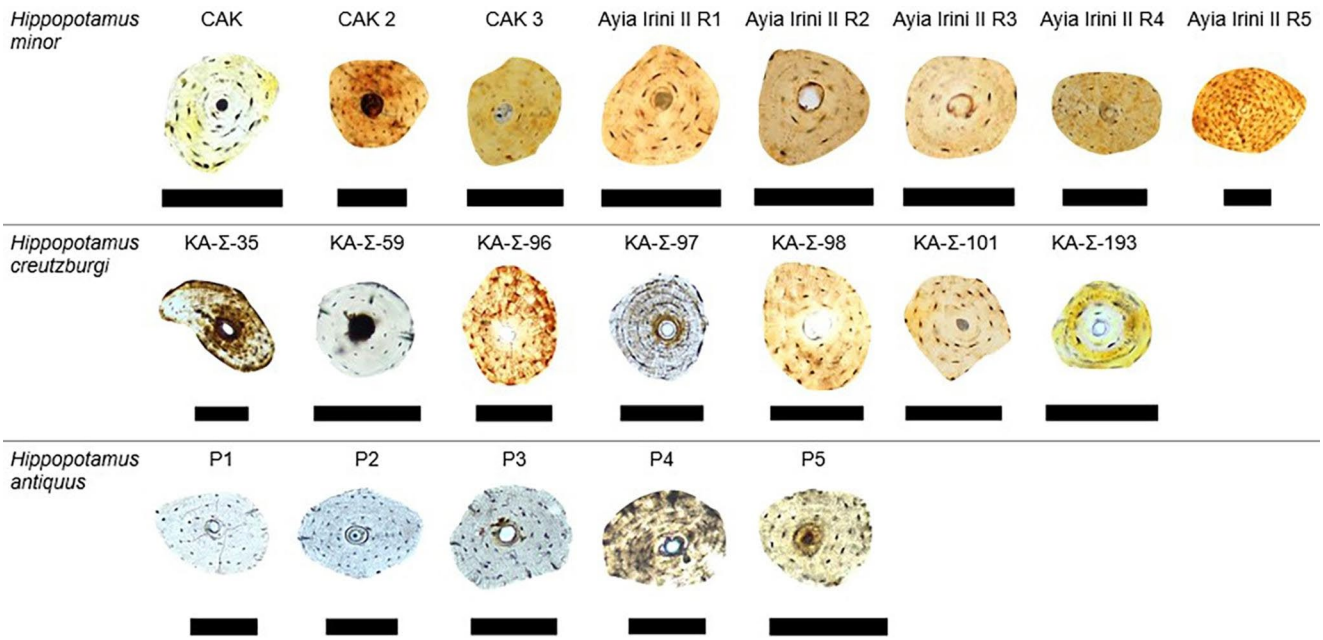

Fig. 4 Representative osteons examined in this study (out of 864 total). Specimen information is as follows: *Hippopotamus minor*: CAK, superior osteon #9 from ROI 3; CAK 2, superior osteon #4 from ROI 2; CAK 3, superior osteon #4 from ROI 3; Ayia Irini II R1, cutaneous osteon #3 from ROI 1; R2, cutaneous osteon #11 from ROI 1; R3, cutaneous osteon #2 from ROI 3; R4, cutaneous osteon #1 from ROI 3; R5, superior osteon #1 from ROI 3. *Hippopotamus creutzburgi*: KA-Σ-35, pleural osteon #2 from ROI 3; KA-Σ-59, cutaneous osteon #2 from ROI 2; KA-Σ-96, superior osteon #1 from ROI 1; KA-Σ-97, inferior osteon #5 from ROI 1; KA-Σ-98, cutaneous osteon #2 from ROI 2; KA-Σ-101, superior osteon #11 from ROI 3; KA-Σ-193, cutaneous osteon #1 from ROI 1; *H. antiquus* P1, pleural osteon #1 from ROI 2; P2, cutaneous osteon #5 from ROI 1; P3, cutaneous osteon #3 from ROI 2; P4, osteon #1 from ROI 3 from unidentifiable region; and P5, osteon #3 from ROI 2 from unidentifiable region. In all instances, the term "osteon" refers to to secondary osteon. Scale bars equal 200 µm

Next, each secondary osteon was imported back into ImageJ/Fiji and measured for secondary osteon area (On.Ar) (also using the "Freehand selection" tool in Fiji/ImageJ; Miszkiewicz and van der Geer 2022), and osteocyte lacuna number (Ot.N, using the "Multi-point" tool; Miszkiewicz et al. 2020) (Fig. 1). The raw Ot.N were converted into densities by dividing the counts by secondary osteon area generating a new osteocyte lacuna density (Ot.Dn) variable (see Bromage et al. 2009; Miszkiewicz et al. 2020) (Fig. 1). The Ot.Dn data were divided by Rib.dm to account for any confounding effects of rib size on the underlying osteocyte lacunae data.

We minimised any observer errors in data collection by taking repeat measurements of On.Ar and Ot.Dn a month following the main phase of data collection and evaluating whether there are statistically significant differences in the data using a paired samples *t*-test applied to 20 re-analysed images. We used Past 4.05b (Hammer et al. 2001) for all statistical analyses. We correlated Ot.N with On.Ar using Pearson's *r* to check whether secondary osteon size related to the osteocyte lacuna number. We then applied non-parametric tests for our species comparisons because of sample size < 10 in all three species groups. Due to a lack of individual weights for animals in each species, we compared data using a Kruskal-Wallis test with a Mann Whitey *U* paired post-hoc identifying specific pairs instead of regressing Ot.Dn against body mass. Next, Ot.Dn data alone first, and then repeated on Ot.Dn data adjusted by Rib.dm were analysed. For the latter, we had to exclude the *H. antiquus* specimens due to their fragmentation. We used the standard alpha value of 0.05 to indicate statistical significance, but also included a Bonferroni correction considering two repeated tests as multiple testing ($p \leq 0.025$).

Results

No statistically significant differences in the intra-observer measurements were noted (Online Resource 2). The rib shaft size ranged from 10 to 23.1 mm, with a mean of 14.8 mm reflecting the variation in rib size across the three species in our total sample (Table 2). The mean rib diameter was 13.6 mm in *H. minor*, 17 mm in *H. creutzburgi*, and 13.9 mm *H. antiquus*. We remind the *H. antiquus* rib piece measurements are not reflective of intact shaft cross-sections given their fragmentation. The rib cross-sections were

Table 2 Summary of rib characteristics, including inferior-superior diameter (Rib.dm) and histomorphological features of the medullary cavity (RT: regular trabeculae: ≥ 5 spicules, ST: sporadic trabeculae: ≤ 4 spicules, EC: empty cavity), bone tissue and secondary osteon traits, and number of "super" osteons (measuring ≥ 100,000 μm^2; Nganvongpanit et al. 2017; Basilia et al. 2023b) observed in this study. Abbreviations: **n/a**, not applicable; **x**, observed; **-**, not observed

Species	Specimen ID	Rib.dm (mm)	Medullary cavity	Widespread Haversian bone	Multiple osteon generations	Resorption cavities	Incompletely filled osteons	Embedded osteons	"Super" osteons
Hippopotamus minor	Akanthou CAK	13.1	x, RT	x	x	x	x	x	2
	Akanthou CAK 2	14.6	x, EC	x	x	x	x	x	4
	Akanthou CAK 3	13.9	x, ST	x	x	x	x		1
	Ayia Irini II R1	12.7	x, ST	x	x	x	x	x	3
	Ayia Irini II R2	14.1	x, RT	x	x	x		x	0
	Ayia Irini II R3	13.6	x, RT	x	x	x	x	x	0
	Ayia Irini II R4	14.3	x, ST	x	x	x	x	x	2
	Ayia Irini II R5	12.6	x, ST	x	x		x	x	2
	Average	**13.6**						**Total**	**14**
Hippopotamus creutzburgi	KA-Σ-35	16.0	x, ST	x	x		x	x	6
	KA-Σ-59	16.2	x, EC	x	x			x	1
	KA-Σ-96	15.7	x, ST	x	x	x		x	2
	KA-Σ-97	17.8	x, EC	x	x	x	x	x	2
	KA-Σ-98	16.7	x, ST	x	x	x		x	6
	KA-Σ-101	19.5	x, RT	x	x			x	0
	KA-Σ-193	16.9	x, ST	x	x	x	x	x	0
	Average	**17**						**Total**	**17**
Hippopotamus antiquus	P1	23.1	n/a*	x	x		x	x	9
	P2	12.2		x	x			x	0
	P3	14		x	x			x	0
	P4	10		x	x			x	2
	P5	10		x	x			x	2
	Average	**13.9**						**Total**	**13**

*fragmented rib pieces

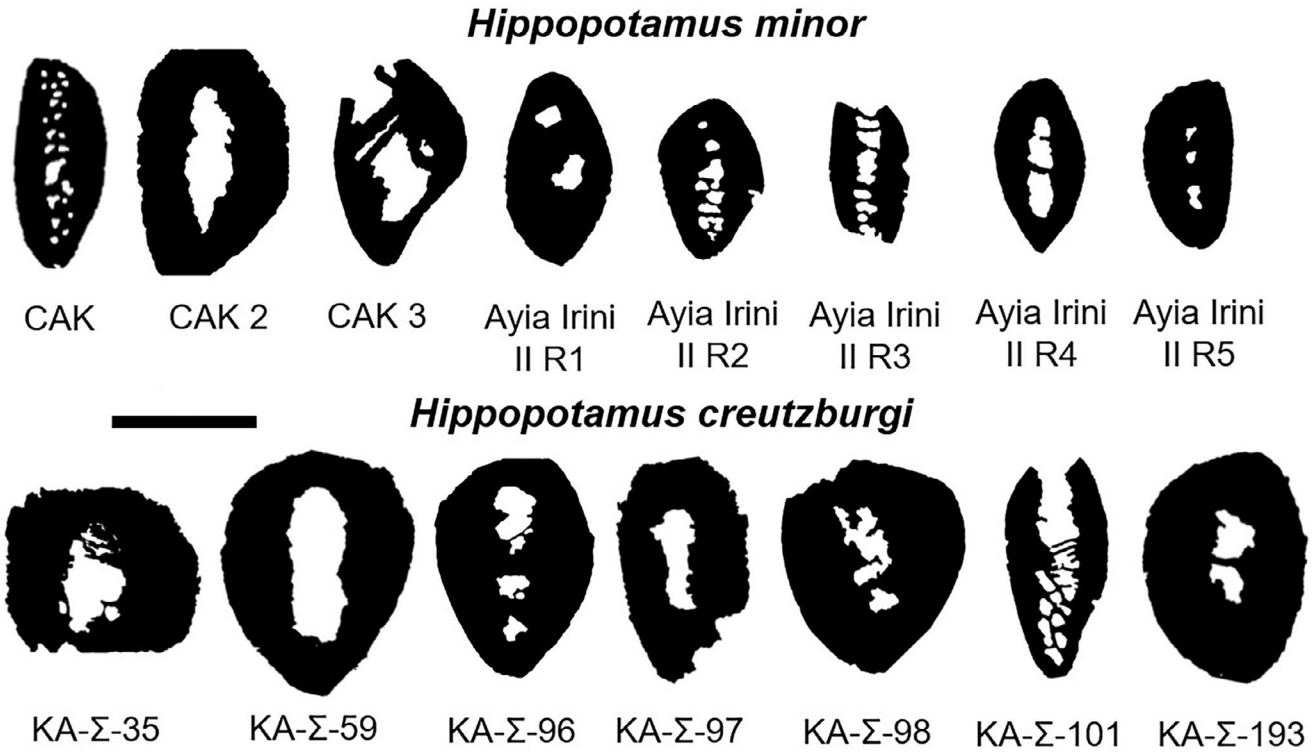

Fig. 5 Outlines of rib cross sections of *Hippopotamus minor* and *H. creutzburgi*. Medullary cavity, sometimes filled with trabeculae, can be seen in every single rib section in both species. All outlines in this figure are arranged so that the caudal aspect is towards the bottom of each image panel, the cranial aspect is towards the top of each panel. Scale bar equals 1 cm

mostly consistently similar in shape, ranging from oval to more circular in *H. minor* and *H. creutzburgi* (Fig. 5). A notable structural bone composition is that all of the ribs with intact cross-sections showed a clear medullary feature partially filled with trabeculae, though at least four rib slides had "empty" cavities (Fig. 5). This is a heterogenous pattern where the empty cavities appear in rib sections with thicker cortices, whereas the multiple trabeculae associated with thinner cortices (NB. it is also possible that fragile trabeculae became damaged during taphonomic fragmentation of the assemblage). All thin sections exhibited complete coverage of well-remodelled Haversian bone with several generations of remodelling as indicated by presence of fragmented and intact secondary osteons (Fig. 6). In addition, 14 slides exhibited "super osteons" which measured $\geq 100{,}000$ µm ^{2} (Nganvongpanit et al. 2017; Basilia et al. 2023b), which also occurred regardless of the species considered (total of 14, 17 and 13 "super" osteons observed in *H. minor*, *H. creutzburgi*, and *H. antiquus*, respectively) (Table 2). In eleven (out of 20) slides there were very clear multiple resorption cavities. Every single slide but one showed embedded secondary osteon variants (Cooke et al. 2022) where new secondary osteons had formed within the central canal of the older generations of secondary osteons (Fig. 6).

A total of 864 secondary osteons were examined. The area of secondary osteons ranged from 4,375 µm^2 to 185,819 µm^2, averaging 46,855 µm^2 per secondary osteon, but increasing in size from the smallest in *H. minor* to the largest in *H. antiquus* (Table 3, Online Resource 3). The total number of osteocyte lacunae across all three samples was 43,357, averaging 50 lacunae per secondary osteon (Table 3, Online Resource 4). The average raw number of osteocyte lacunae was almost the same in *H. minor* and *H. creutzburgi*, but lower in *H. antiquus* (Table 3, Online Resource 4). There was a strong positive correlation between the raw number of osteocyte lacuna counts and the area of secondary osteons ($r = 0.809$, $p = 0.0001$), such that larger secondary osteons had higher counts of osteocyte lacunae (Table 3; Fig. 7).

Once Ot.Dn was computed, it became clear that it presented with a gradient along the body mass increase with the highest Ot.Dn in the ribs from the smallest *H. minor*, intermediate values in the intermediate size *H. creutzburgi*, and the lowest values in the largest *H. antiquus* (Table 3, Online Resource 5). A Kruskal-Wallis test returned statistically significant differences between the three groups ($ch^2 = 11.77$, $p = 0.003$). Mann Whitney *U* pairwise comparisons identified *H. creutzburgi* ($p = 0.009$) and *H. minor* ($p = 0.004$) data to be statistically significantly different from *H. antiquus*. Once Ot.Dn was adjusted by Rib.dm (excluding *H. antiquus*), these differences became more pronounced between *H. creutzburgi* from *H. minor* (Kruskal-Wallis: $ch^2 = 11.54$, $p = 0.003$) (Fig. 8). Pairwise Mann-Whitney *U* comparisons

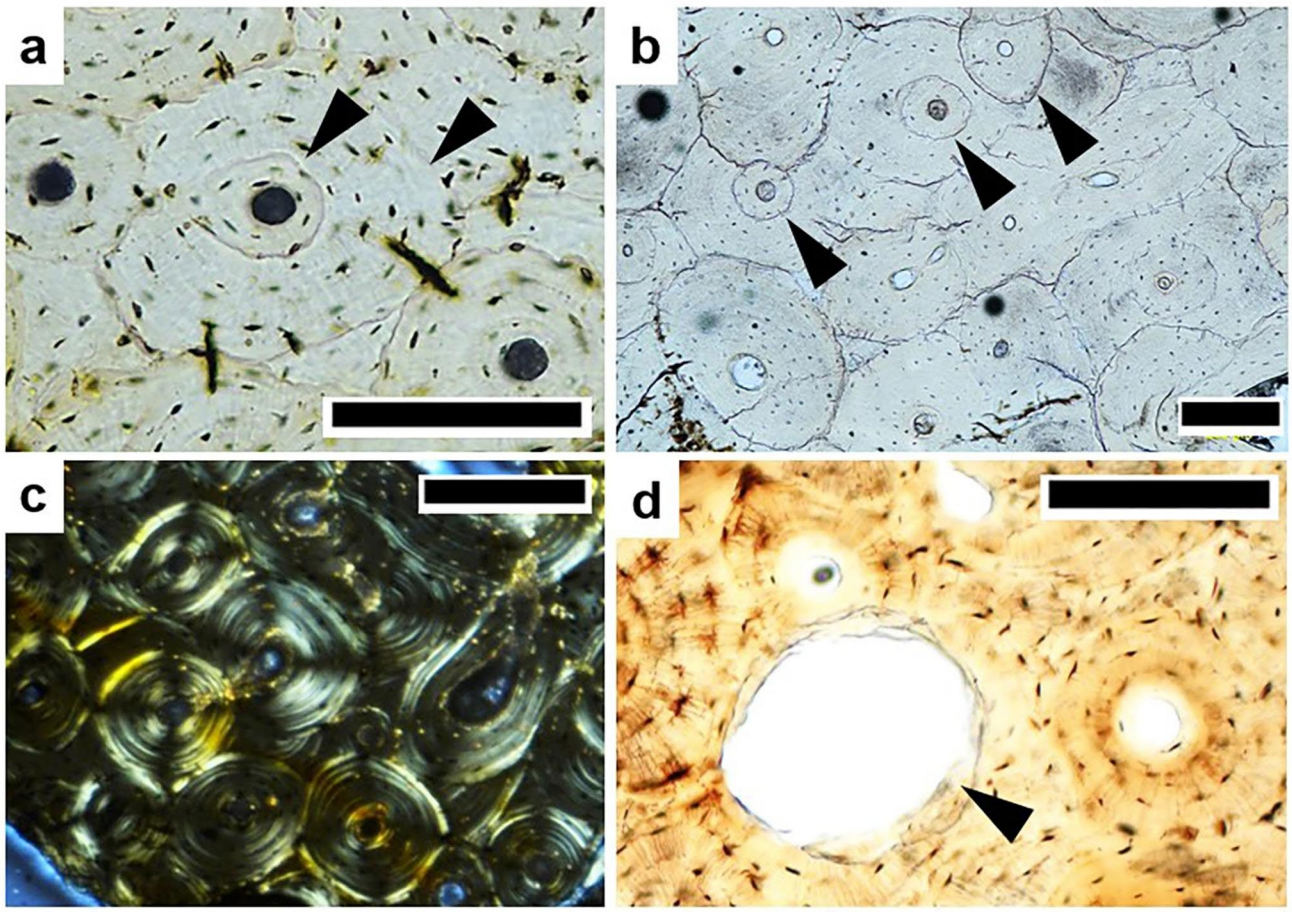

Fig. 6 Osteon micrographs with arrowheads indicating different osteon types, Haversian bone features, and resorption spaces. **a**. embedded osteon from the inferior rib region in *H. minor* (specimen ID: CAK); **b**. embedded osteons in rib pleural area from *H. antiquus* (specimen ID: P1); **c**. dense Haversian bone in *H. minor* (specimen ID: CAK) under polarised light, inferior region; **d**. resorption cavity in *H. creutzburgi* (specimen ID: KA-Σ-98), rib cutaneous area. Scale bars equal 200 µm

Table 3 Descriptive and inferential statistics per rib (based on *Hippopotamus* species averages). For data presented by specimens within species, see Online Resources 3–6. The correlation statistics are for individual pairs of 864 secondary osteons and related osteocyte lacunae

Species	Variable	Mean	Max	Min	SD	Statistics
H. minor	Ot.N (number)	52.9	67.4	38.3	10.7	$r=0.877$, $p=0.0001$*
	On.Ar (µm^2)	43,783.6	56,733.6	31,962.6	9,359.1	
	Ot.Dn (number/mm^2)	1,324	1,707.7	1,001.7	212.1	*H. creutzburgi* ($U=14$, $p=0.118$), *H. antiquus* ($U=0$, $p=0.004$*)
	Ot.Dn/Rib.dm	97.7	125.8	76.5	5.5	*H. creutzburgi* ($U=2$, $p=0.003$), *H. antiquus* ($U=2$, $p=0.010$*)
H. creutzburgi	Ot.N (number)	50.5	66.5	34.9	10	$r=0.847$, $p=0.0001$*
	On.Ar (µm^2)	46,788.1	60,179.7	35,443.9	9,206.2	
	Ot.Dn (number/mm^2)	1,159.1	1,546.7	905.27	219.2	*H. minor* (as above), *H. antiquus* ($U=1$, $p=0.009$*)
	Ot.Dn/Rib.dm	68.3	80.5	53.6	11.2	*H. minor* (as above), *H. antiquus* ($U=16$, $p=0.871$)
H. antiquus	Ot.N (number)	43.3	54.9	31.5	10.6	$r=0.915$, $p=0.0001$*
	On.Ar (µm^2)	60,480.4	75,866.9	38,233.8	18,974	
	Ot.Dn (number/mm^2)	783.6	953.3	656.7	107.9	*H. minor* (as above), *H. creutzburgi* (as above)
	Ot.Dn/Rib.dm	62.9	78.1	28.4	21.2	

*values are statistically significant both at alpha = 0.05 and when Bonferroni correction is applied ($p \leq 0.025$)

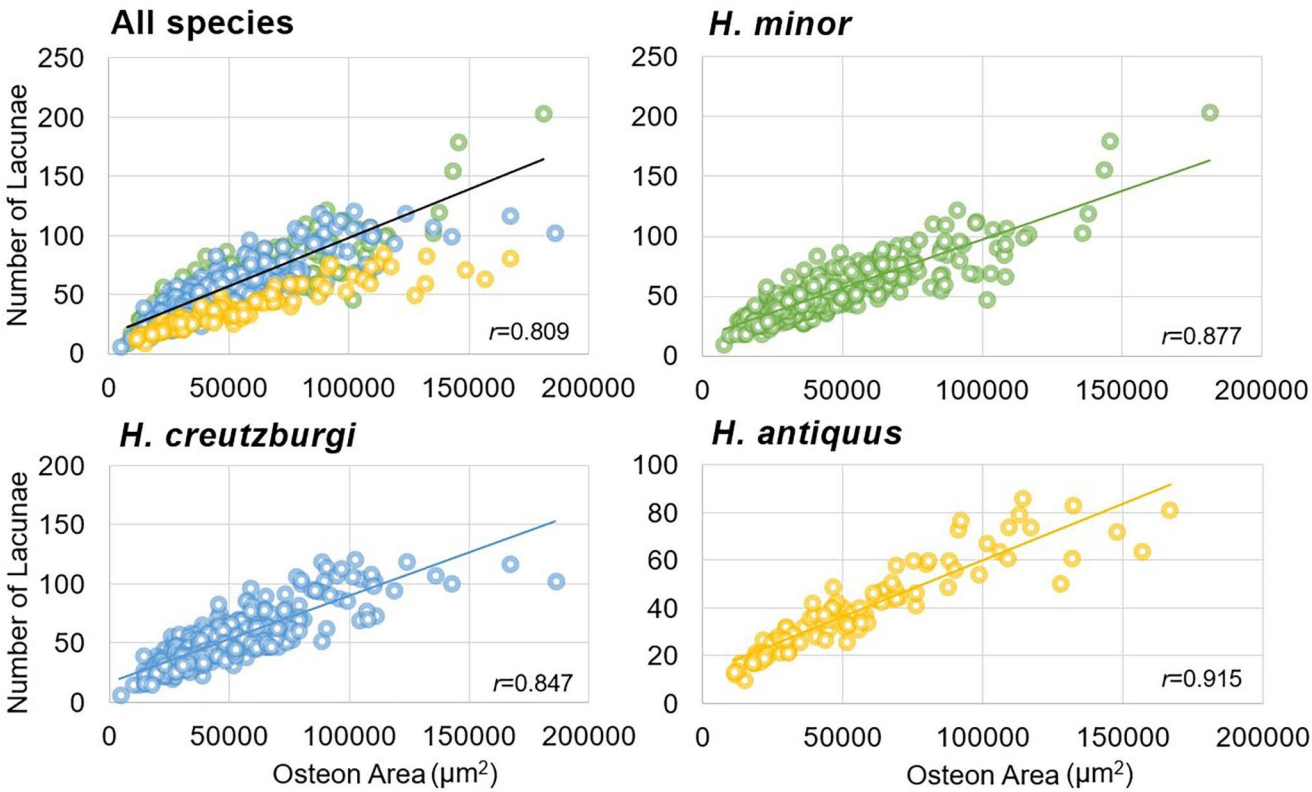

Fig. 7 Summary correlations between raw osteocyte lacuna counts and related secondary osteon area. In all cases, $p = 0.0001$

revealed higher Ot.Dn/Rib.dm in *H. minor* than in *H. creutzburgi* ($p = 0.003$).

Discussion

Osteocyte lacuna densities in the secondary osteons differed between adult *Hippopotamus* species of different body masses in our study. This finding confirmed our prediction that the smallest *H. minor* would have the highest densities of osteocyte lacunae, but the trend would be opposite in the largest *H. antiquus*, likely relating to accelerated life history (Sibly and Brown 2007) in the dwarfed hippopotamus.

The pattern in our results is consistent with osteocyte lacuna data in prior publications considering pygmy hippopotamuses (Bromage et al. 2009) and giant rats (Miszkiewicz et al. 2020). Although these prior studies examined lamellar bone in long bones rather than individual secondary osteons, the trend in osteocyte lacuna densities changing along the body size gradient is similar. We worked with individual secondary osteons because each one reflects a single BMU event operating in a mature skeleton (Ryser et al. 2009). As a result, data in our study offer an insight into bone remodelling relating to short-term physiological cycles of rib bone maintenance that the hippopotamuses represented here experienced under insular and mainland conditions. Because we also examined ribs rather than limb bones, we can assume that the osteocyte lacuna densities and secondary osteon morphologies were not completely stimulated by mechanical stresses, but likely reflected stochastic remodelling (Stewart et al. 2021; see also Smit 2021). Thus, our data should reflect basic bone physiological "signals" that clearly differ between the three species, or between island/ mainland conditions, or different body size classes. Our main interpretation is that, relative to the other two hippopotamuses of larger body mass, the highest osteocyte lacuna densities in the smallest hippopotamus ribs reflect the corresponding number (i.e., also the highest) of osteoblasts operating at each BMU event (Chang and Liu 2022). Osteoblasts convert to osteocytes within a matter of days as osteoid (immature bone matrix) becomes mineralised during osteon formation (Qiu et al. 2003), so the density of osteocyte lacune is a very good proxy for the number of osteocytes (and thus, osteoblasts) being entrapped during BMU activity (Bromage et al. 2009; however, we acknowledge some portion of osteoblasts ceases due to cell apoptosis; see Parfitt 1994). This indicates that a smaller (insular) hippopotamus skeleton (or at least its ribs) might have evolved faster remodelling (reflecting skeletal metabolism), than that of its larger mainland counterpart, to ensure optimised calcium homeostasis in the face of body size reduction. In other words, a higher number of osteoblasts (which are then converted to osteocytes) are needed

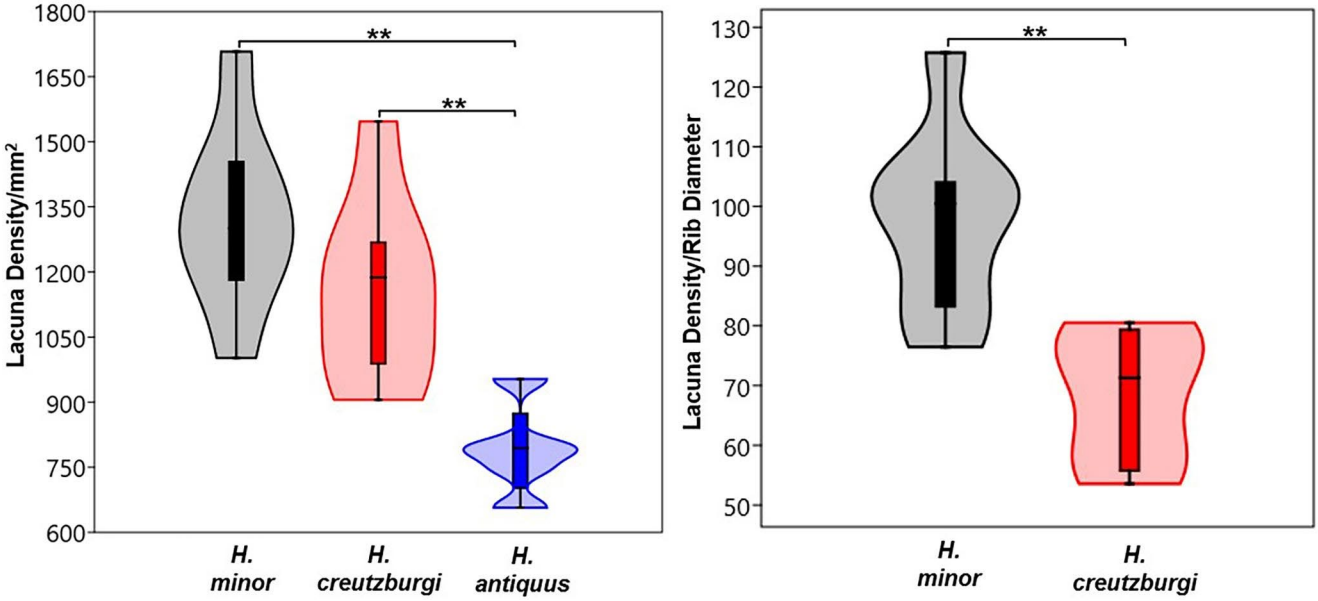

Fig. 8 Violin and box plots summarising osteocyte lacunae in the three species examined (left), and the same data adjusted by inferior-superior rib diameter in *Hippopotamus minor* and *H. creutzburgi* (right). The double asterisks (**) indicate $p < 0.01$

to create an osteon during a BMU event, which is designed for molecular exchanges ensuring bone homeostasis (Qiu et al. 2003), in a relatively short period of time because a smaller mammal grows quicker than a large mammal (Bromage et al. 2009). Our raw osteocyte lacuna number (prior to density calculation) correlated very strongly and positively with secondary osteon size (see Fig. 7), whereby large secondary osteons had relatively high lacuna counts. This suggests that the quantum of bone generated in one BMU remodelling event was proportional to osteocyte/osteoblast activity, forming optimal final secondary osteons in terms of bone quality (in all three species *r* ranged 0.877–0.915). This suggests each BMU achieving bone homeostasis (Chang and Liu 2022), and confirming our data represent physiological processes rather than originating from pathological or biomechanical stimulation. Otherwise, greater osteocyte lacuna counts could be expected in smaller secondary osteons (*inverse* relationship) indicating an inhibition of bone formation (numerous osteoblasts but impaired bone production) (Skedros et al. 2011) – we would have observed negative correlations between secondary osteon size and osteocyte lacuna counts. In addition to the *direct* relationships we found in the hippopotamus samples, Skedros et al. (2011) confirmed they may also exist in human ribs; calcanei from sheep, deer, elk, horses; and radii and metacarpals in horses.

The implications of our study are limited to adult hippopotamuses only because we focussed on secondary osteons in completely remodelled cortices. We did not have access to juvenile specimens, or older specimens with sporadically occurring Haversian bone, where the density of osteocyte lacunae could be examined across primary bone regions, as was done in the studies by Bromage et al. (2009) and Miszkiewicz et al. (2020), and where clear transitions between primary vessels and secondary osteons could be examined pinpointing stages at which bone remodelling started operating in bones and individuals (Pitfield et al. 2017). Examining bone remodelling patterns in juvenile specimens could have provided further insights into the trend of bone metabolic changes at different ontogenetic stages of insular dwarf species. The prior bone histology descriptions by Kolb et al. (2015) clearly suggested modification of bone growth in a small sample of insular juvenile hippopotamuses (*H. minor*), which our new Haversian bone data complement. Future osteocyte lacuna data from larger sample sizes of juvenile specimens will further expand these attempts to characterise bone modelling and remodelling in hippopotamuses from different island environments with different ecologies and degrees of body mass shifts.

For the extinct dwarf hippopotamuses considered in our study, the shift from mainland to insular environments must have triggered a range of biological changes, so clearly reflected in the extreme degree of body size change down to 13% (*H. creutzburgi*) and 4% (*H. minor*) of the ancestral mass as estimated based on long bones (Lomolino et al. 2013). As these species underwent a significant body size reduction, the regulation of their organisms' needs needed to continue, which is why bone remodelling, likely one of multiple other metabolic processes, adjusted to this shift. Working with fossil specimens limits our discussion around metabolism more broadly (defined as converting food into energy for growth and reproduction; see McNab 2019), but

bone remodelling is recognised as one of metabolic processes maintaining bone tissue structure and facilitating response to environmental stimuli (Robling et al. 2006; Qin et al. 2020). Further, regulation of bone mass in mammals has been proposed to link with energy metabolism via leptin (appetite suppressing hormone), although these insights are still based on observational data in rats, mice, and humans (see review by Karsenty and Khosla 2022). Once the nature of the biochemical cross-talk between leptin and bone mass is unravelled, differences in bone remodelling between hippopotamuses of different skeletal sizes in insularity contexts could provide a new means for palaeontological reconstructions of energy metabolism in extinct mammal taxa. Hippopotamuses are excellent candidates for this type of research because both the common and pygmy hippopotamuses are thought to have very low energy requirements and basal metabolic rates (BMR) (Schwarm et al. 2006), at least in captivity (Schwarm et al. 2006; Taylor et al. 2013). Schwarm et al. (2006) in fact found no differences in average digestibility when comparing eight captive *H. amphibius* (n = 4) and *C. liberiensis* (n = 4). Given that the modern *C. liberiensis* is not an insular dwarf species, and the captive nature of the Schwarm et al.'s (2006) study, we could propose that the species differences in bone remodelling in our samples may relate to insularity and non-captivity, along with the extinct Mediterranean hippopotamuses being more terrestrial than semi-aquatic. This can be framed from the perspective of a cross-talk between bone and energy metabolism (Confavreux et al. 2009). Schwarm et al. (2006) discussed a hypothesis that species-specific low energy needs in hippopotamuses could relate to energy investment into growth and reproduction, and adaptability when occupying various environmental niches. A reduced body size in an insular pygmy mammal would probably require maximising of energy consumption, as per life history theory, to optimise reproduction and growth under insularity conditions, and as a result of a shift in surface-volume ratio (Palkovacs 2003).

Aside from bone remodelling data, our study also characterised some new hippopotamus bone histology observations that are worth noting for palaeontologists. All the rib cross-sections were similar in shape, and exhibited medullary cavity filled with partial spongiosa as reported in previous research by Hayashi et al. (2013) and Houssaye et al. (2016a, b; 2021). The widespread Haversian bone with a series of secondary osteon variants, including embedded ones, and some instances of the onset of resorption as inferred from the occurrence of resorption cavities, indicate active remodelling in the ribs of hippopotamuses in our study regardless of the species considered. We also observed the presence of "super" secondary osteons which have so far been noted only in Asian elephants (Nganvongpanit et al. 2017; Basilia et al. 2023a, b). These super secondary osteons simply refer to the existence of unusually large secondary osteon surfaces indicating prolonged action of osteoclasts which leads to secondary osteon expansion in terms of the space it occupies within cortex (Nganvongpanit et al. 2017; Basilia et al. 2023a, b). We hypothesise the occurrence of these osteon variants could be a feature of very large mammals, particularly in the context of the Felder et al's (2017) allometry findings of secondary osteon and body size in various mammals. Apparently, as we have shown here for hippopotamuses, this feature is retained in descendant species (*H. creutzburgi, H. minor*) of the same species (*H. antiquus*) that evolved a body mass similar to pigs, which might imply that Felder et al.'s (2017) allometric rule does not necessarily apply to phyletic insular dwarfs. This conclusion is, however, cautionary, because first of all, our study is limited to three species only, and secondly, no large-scale investigation on the presence of super secondary osteons throughout the mammalian phylogeny has been undertaken.

Aside from the small sample size, a limitation impacting our results involves the inclusion of Haversian canals in the secondary osteon area measurements. We acknowledge that the space taken up by a central canal could have a dimensional effect on the secondary osteon size. We did, however, ensure that the secondary osteons were at a completed stage, and our research question centred on the size that a BMU forms through resorption by osteoclast cells, which is the overall measure as deduced by tracing secondary osteon cement lines. Further, this study only worked with fossil specimens, so we assume that the complete secondary osteons are the youngest, or the latest, remodelling events in each rib. The fragmentation of the ribs limited our histology analysis, which also meant our comments about the rib cross-section shape are restricted to the rib location we sectioned. Having said this, the use of ribs proved useful confirming prior observations that rib histology can help future studies elucidate intricate biological processes occurring in bone of insular fossil mammals.

Conclusions

We found that rib histology in the smallest hippopotamus to have ever existed, the Pleistocene *H. minor* from Cyprus, had much higher densities of osteocyte lacunae at the level of secondary osteons, when compared to ribs from larger hippopotamuses, *H. creutzburgi* of Crete (Greece) and *H. antiquus* (mainland Greece). Osteocyte lacuna densities distinctly separated these three species, possibly signifying a gradient in bone remodelling where bone tissue optimises its maintenance to achieve homeostasis in the face of insularity driven reduction of body size. Our findings add

further support to previously observed trends in osteocyte lacunae increasing in densities along with decreasing body mass in extant pygmy and common hippopotamuses (Bromage et al. 2009), and giant and common murines (Miszkiewicz et al. 2020). Future examination of osteocyte lacuna densities in palaeontological contexts can help elucidate intricate biological processes that occur in bone of insular fossil mammals.

Supplementary information The online version contains supplementary material available at https://doi.org/10.1007/s10914-023-09688-y.

Acknowledgements We thank David McGregor (Australian National University), Kelvin Henderson (University of Queensland), Dirk van der Marel, Hanco Zwaan, and Elza Duijm (Naturalis Biodiversity Center) for technical assistance and facilitating laboratory access during histology preparation and image acquisition. JJM thanks Martin Rücklin for facilitating office access during the Martin & Temminck Fellowship and Thirza de Kruijff for coordinating the fellowship at Naturalis Biodiversity Center. AG thanks Michael Dermitzakis (National and Kapodistrian University of Athens) for providing access to their *Hippopotamus* collection. We thank Christian Kolb for additional information on the Cyprus hippopotamus. We are grateful to Darin Croft, Brandon Kilbourne, Alexandra Houssaye, and an anonymous reviewer, for their constructive feedback on our article.

Author contributions All authors contributed to the study conception and design. Material preparation was performed by Athanassios Athanassiou, George A. Lyras, and Alexandra van der Geer. Data collection and analysis were performed by Justyna J. Miszkiewicz and Alexandra van der Geer. The first draft of the manuscript was written by Justyna J. Miszkiewicz and all authors commented on previous versions of the manuscript. All authors read and approved the final manuscript.

Funding Open Access funding enabled and organized by CAUL and its Member Institutions. Funding was received from Naturalis Biodiversity Center under a Martin & Temminck Fellowship grant.

Data Availability Data are available open access from Figshare https://doi.org/10.6084/m9.figshare.23884497. Histology samples are retained part of the main collections.

Declarations

Ethics approval and consent to participate Approval to conduct this research was issued by the Department of Geology and Geoenvironment at National and Kapodistrian University of Athens and the Ephorate of Palaeoanthropology and Speleology of the Ministry of Culture of Greece.

Competing interests The authors have no competing interests to declare.

References

Adams NF, Candy I, Schreve DC (2022) An Early Pleistocene hippopotamus from Westbury Cave, Somerset, England: support for a previously unrecognized temperate interval in the British Quaternary record. J Quat Sci 37:28–41. https://doi.org/10.1002/jqs.3375

Basilia P, Miszkiewicz JJ, Nganvongpanit K, Zaim J, Rizal Y, Aswan, Puspaningrum MR, Trihascaryo A, Price GJ, van der Geer AA, Louys J (2023a) Bone histology in a fossil elephant (*Elephas maximus*) from Pulau Bangka, Indonesia. Hist Biol 35:8:1356–1367. https://doi.org/10.1080/08912963.2022.2092850

Basilia P, Miszkiewicz JJ, Zaim J, Rizal Y, Aswan, Pupangingrum MR, Tri Hascaryo A, Price GJ, Louys J. (2023b) Investigating super osteons in fossil Asian elephant (*Elephas maximus)* bone from Bangka Island, southeast Sumatra. In: Louys J, van der Geer AAE, Albers PCH (eds) Quaternary Palaeontology and Archaeology in Sumatra. ANU Press, Canberra, pp xx-xx (in press)

Benítez-López A, Santini L, Gallego-Zamorano J, Milá B, Walkden P, Huijbregts MA, Tobias JA (2021) The island rule explains consistent patterns of body size evolution in terrestrial vertebrates. Nat Ecol Evol 5:768–86. https://doi.org/10.1038/s41559-021-01426-y

Boekschoten GJ, Sondaar PY (1966) The Pleistocene of the Katharo Basin (Crete) and its hippopotamus. Bijdr Dierkd 36:17–42.

Boekschoten GJ, Sondaar PY (1972) On the fossil Mammalia of Cyprus, I & II. Proc Kon Ned Akad Wetensch Ser B 75:306–38.

Bromage TG, Lacruz RS, Hogg R, Goldman HM, McFarlin SC, Warshaw J, Dirks W, Perez-Ochoa A, Smolyar I, Enlow DH, Boyde A (2009) Lamellar bone is an incremental tissue reconciling enamel rhythms, body size, and organismal life history. Calcif Tiss Int 84:388–404. https://doi.org/10.1007/s00223-009-9221-2

Chang B, Liu X (2022) Osteon: structure, turnover, and regeneration. Tissue Eng Part B Rev 28:261–278. https://doi.org/10.1089/ten.teb.2020.0322

Confavreux CB, Levine RL, Karsenty G (2009) A paradigm of integrative physiology, the crosstalk between bone and energy metabolisms. Mol Cell Endocrinol 310:21–29. https://doi.org/10.1016/j.mce.2009.04.004

Cooke KM, Mahoney P, Miszkiewicz JJ (2022) Secondary osteon variants and remodeling in human bone. Anat Rec 305:1299–315. https://doi.org/10.1002/ar.24646

Cooper LN, Clementz MT, Usip S, Bajpai S, Hussain ST, Hieronymus TL (2016) Aquatic habits of cetacean ancestors: integrating bone microanatomy and stable isotopes. Integr Comp Biol 56:1370–1384 https://doi.org/10.1093/icb/icw119

Currey JD, Dean MN, Shahar R (2017) Revisiting the links between bone remodelling and osteocytes: insights from across phyla. Biol Rev 92:1702–1719. https://doi.org/10.1111/brv.12302

Dempster DW, Compston JE, Drezner MK, Glorieux FH, Kanis JA, Malluche H, Meunier PJ, Ott SM, Recker RR, Parfitt AM (2013) Standardized nomenclature, symbols, and units for bone histomorphometry: a 2012 update of the report of the ASBMR Histomorphometry Nomenclature Committee. J Bone Miner Res 28:2–17. https://doi.10.1002/jbmr.1805

Deraniyagala PE (1955) The extinct *Hippopotamus antiquus* of Europe. Spol Zeylan 27:219–223.

Dietrich WO (1928) Pleistocäne Deutsch–Ostafrikanische *Hippopotamus*–reste. Wissensch Ergebnisse Oldoway Exped Herausgeben 3:1–41.

Faure M (1981) Répartition des Hippopotamidae (Mammalia, Artiodactyla) en Europe occidentale implications stratigraphiques et paléoécologiques. Geobios 14(2):191–200.

Felder AA, Phillips C, Cornish H, Cooke M, Hutchinson JR, Doube M (2017) Secondary osteons scale allometrically in mammalian humerus and femur. R Soc Open Sci 4:170431. https://doi.org/10.1098/rsos.170431

Francillon-Vieillot H, de Buffrénil V, Castanet J, Géraudie J, Meunier FJ, Sire JY, Zylberberg L. de Ricqlès A (1990) Microstructure and mineralization of vertebrate skeletal tissues. In: Carter JG (ed) Skeletal Biomineralization: Patterns, Processes and Evolutionary Trends. Van Nostrand, New York, pp 471–547.

Fröhlich J, Kubickova S, Musilova P, Cernohorska H, Muskova H, Rubes J (2017) A comparative study of pygmy hippopotamus (*Choeropsis liberiensis*) karyotype by cross-species chromosome painting. J Mamm Evol 24:465–74. https://doi.org/10.1007/s10914-016-9358-5

Frost HM (2001) From Wolff's law to the Utah paradigm: insights about bone physiology and its clinical applications. Anat Rec 262:398–419. https://doi.org/10.1002/ar.1049

Georgitsis MK, Liakopoulou DE, Theodorou GE (2022) Morphofunctional examination of the carpal bones of pygmy hippopotamus from Ayia Napa, Cyprus. Anat Rec 305:297–320. https://doi.org/10.1002/ar.24738

Gray NM, Kainec K, Madar S, Tomko L, Wolfe S (2007) Sink or swim? Bone density as a mechanism for buoyancy control in early cetaceans. Anat Rec 290:638–53. https://doi.org/10.1002/ar.20533

Hammer Ø, Harper DA, Ryan PD. PAST: Paleontological statistics software package for education and data analysis. Palaeontol Electron 4.1.4A:1–9.

Hart NH, Newton RU, Tan J, Rantalainen T, Chivers P, Siafarikas A, Nimphius S (2020) Biological basis of bone strength: anatomy, physiology and measurement. J Musculoskelet Neuronal Interact 20:347–371.

Hayashi S, Houssaye A, Nakajima Y, Chiba K, Ando T, Sawamura H, Inuzuka N, Kaneko N, Osaki T (2013) Bone inner structure suggests increasing aquatic adaptations in Desmostylia (Mammalia, Afrotheria). PLoS One 8(4):e59146. https://doi.org/10.1371/journal.pone.0059146

Houssaye A, Fernandez V, Billet G. (2016a) Hyperspecialization in some South American endemic ungulates revealed by long bone microstructure. J Mamm Evol 23:221–35. https://doi.org/10.1007/s10914-015-9312-y

Houssaye A, Waskow K, Hayashi S, Cornette R, Lee AH, Hutchinson JR (2016b) Biomechanical evolution of solid bones in large animals: a microanatomical investigation. Biol J Linn 117:350–71. https://doi.org/10.1111/bij.12660

Houssaye A, Martin F, Boisserie JR, Lihoreau F (2021) Paleoecological inferences from long bone microanatomical specializations in Hippopotamoidea (Mammalia, Artiodactyla). J Mamm Evol 28:847–70. https://doi.org/10.1007/s10914-021-09536-x

Karsenty G, Khosla S (2022) The crosstalk between bone remodeling and energy metabolism: A translational perspective. Cell Metab 34:805–817 https://doi.org/10.1016/j.cmet.2022.04.010

Köhler M, Moyà-Solà S (2009) Physiological and life history strategies of a fossil large mammal in a resource-limited environment. Proc Natl Acad Sci USA 106:20354–8. https://doi.org/10.1073/pnas.0813385106

Köhler ME, Pérez-Mellado V, Ramon MM (2010) Fast or slow? The evolution of life history traits associated with insular dwarfing. In: Pérez-Mellado V, Ramon C (eds) Islands and Evolution. Intitut Menorqui d'Estudis, Recerca, pp 261–80.

Kolb C, Scheyer TM, Veitschegger K, Forasiepi AM, Amson E, Van der Geer AA, Van den Hoek Ostende LW, Hayashi S, Sánchez-Villagra MR (2015) Mammalian bone palaeohistology: a survey and new data with emphasis on island forms. PeerJ 3:e1358. https://doi.org/10.7717/peerj.1358

Lomolino MV, van der Geer AA, Lyras GA, Palombo MR, Sax DF, Rozzi R (2013) Of mice and mammoths: generality and antiquity of the island rule. J Biogeogr 40:1427–1439. https://doi.org/10.1111/jbi.12096

Major FCI (1902) On the pigmy *Hippopotamus* from the Pleistocene of Cyprus. Proc Zool Soc Lond 2:238–9 https://doi.org/10.1111/j.1469-7998.1902.tb08223.x

Martinez-Navarro B, Pandolfi L, Medin T, Libsekal Y, Ghinassi M, Papini M, Rook L (2022) The ontogenetic pattern of *Hippopotamus gorgops* Dietrich, 1928 revealed by a juvenile cranium from the one-million-years-old paleoanthropological site of Buia (Eritrea). C R Palevol 21:157–73. https://doi.org/10.5852/cr-palevol2022v21a7

Martino R, Pandolfi L (2022) The Quaternary *Hippopotamus* records from Italy. Hist Biol 34:1146–1156. https://doi.org/10.1080/08912963.2021.1965138

Mazza P (1991) Interrelations between Pleistocene hippopotami of Europe and Africa. Boll Soc Paleont It 30:153–186

McNab BK (2019) What determines the basal rate of metabolism? J Exp Biol 222:jeb205591. https://doi.org/10.1242/jeb.205591

Michaux J, López-Martínez N, Hernández-Pacheco JJ (1996) A 14 C dating of *Canariomys bravoi* (Mammalia Rodentia), the extinct giant rat from Tenerife (Canary Islands, Spain), and the recent history of the endemic mammals in the archipelago. Vie Milieu 46:261–266.

Milne Edwards A (1868) Sur des découvertes zoologiques faites récemment à Madagascar par M. Alfred Grandidier. C R Hebdo Seances Acad Sci 67:1165–1167.

Miszkiewicz JJ, van der Geer AA (2022) Inferring longevity from advanced rib remodelling in insular dwarf deer. Biol J Linn Soc 136:41–58. https://doi.org/10.1093/biolinnean/blac018

Miszkiewicz JJ, Louys J, O'Connor S (2019) Microanatomical record of cortical bone remodeling and high vascularity in a fossil giant rat midshaft femur. Anat Rec 302:1934–40. https://doi.org/10.1002/ar.24224

Miszkiewicz JJ, Louys J, Beck RM, Mahoney P, Aplin K, O'Connor S (2020) Island rule and bone metabolism in fossil murines from Timor. Biol J Linn Soc 129:570–586. https://doi.org/10.1093/biolinnean/blz197

Mullender MG, Huiskes R, Versleyen H, Buma P (1996) Osteocyte density and histomorphometric parameters in cancellous bone of the proximal femur in five mammalian species. J Orthop Res 14:972–979. https://doi.org/10.1002/jor.1100140618

Nganvongpanit K, Siengdee P, Buddhachat K, Brown JL, Klinhom S, Pitakarnnop T, Angkawanish T, Thitaram C (2017) Anatomy, histology and elemental profile of long bones and ribs of the Asian elephant (*Elephas maximus*). Anat Sci Int 92:554–68. https://doi.org/10.1007/s12565-016-0361-y

Orlandi-Oliveras G, Nacarino-Meneses C, Koufos GD, Köhler M (2018) Bone histology provides insights into the life history mechanisms underlying dwarfing in hipparionins. Sci Rep 8:17203. https://doi.org/10.1038/s41598-018-35347-x

Padian K, Lamm ET (2013). Bone Histology of Fossil Tetrapods: Advancing Methods, Analysis, and Interpretation. University of California Press, Berkeley.

Palkovacs EP (2003) Explaining adaptive shifts in body size on islands: a life history approach. Oikos 103(1):37–44. https://doi.org/10.1034/j.1600-0706.2003.12502.x

Parfitt AM (1994) Osteonal and hemi-osteonal remodeling: the spatial and temporal framework for signal traffic in adult human

bone. J Cell Biochem 55:273–286. https://doi.org/10.1002/jcb.240550303
Pitfield R, Miszkiewicz JJ, Mahoney P (2017) Cortical histomorphometry of the human humerus during ontogeny. Calcif Tissue Int 101:148–158. https://doi.org/10.1007/s00223-017-0268-1
Pitfield R, Miszkiewicz JJ, Mahoney P (2019) Microscopic markers of an infradian biorhythm in human juvenile ribs. Bone 120:403–410. https://doi.org/10.1016/j.bone.2018.11.019
Psonis N, Vassou D, Nicolaou L, Roussiakis S, Iliopoulos G, Poulakakis N, Sfenthourakis S (2021) Mitochondrial sequences of the extinct Cypriot pygmy hippopotamus confirm its phylogenetic placement. Zool J Linn Soc 196:979–89. https://doi.org/10.1093/zoolinnean/zlab089
Qin L, Liu W, Cao H, Xiao G (2020) Molecular mechanosensors in osteocytes. Bone Res 8:23. https://doi.org/10.1038/s41413-020-0099-y
Qiu S, Fyhrie DP, Palnitkar S, Rao DS (2003) Histomorphometric assessment of Haversian canal and osteocyte lacunae in different-sized osteons in human rib. Anat Rec 272:520–525. https://doi.org/10.1002/ar.a.10058
Raia P, Barbera C, Conte M (2003) The fast life of a dwarfed giant. Evol Ecol 17:293–312. https://doi.org/10.1023/A:1025577414005
Raia P, Meiri S (2006) The island rule in large mammals: paleontology meets ecology. Evolution 60:1731–42. https://doi.org/10.1111/j.0014-3820.2006.tb00516.x
Robling AG, Castillo AB, Turner CH (2006) Biomechanical and molecular regulation of bone remodeling. Annu Rev Biomed Eng 8:455 – 98. https://doi.org/10.1146/annurev.bioeng.8.061505.095721
Ryser MD, Nigam N, Komarova SV (2009) Mathematical modeling of spatio-temporal dynamics of a single bone multicellular unit. J Bone Miner Res 24:860–70. https://doi.org/10.1359/jbmr.081229
Schwarm A, Ortmann S, Hofer H, Streich WJ, Flach EJ, Kühne R, Hummel J, Castell JC, Clauss M (2006) Digestion studies in captive Hippopotamidae: a group of large ungulates with an unusually low metabolic rate. J Anim Physiol Anim Nutr 90:300–308. https://doi.org/10.1111/j.1439-0396.2005.00599.x
Sibly RM, Brown JH (2007) Effects of body size and lifestyle on evolution of mammal life histories. Proc Natl Acad Sci USA 104:17707–12. https://doi.org/10.1073/pnas.0707725104
Skedros JG, Clark GC, Sorenson SM, Taylor KW, Qiu S (2011) Analysis of the effect of osteon diameter on the potential relationship of osteocyte lacuna density and osteon wall thickness. Anat Rec 294:1472–1485. https://doi.org/10.1002/ar.21452
Smit TH (2021) Closing the osteon: Do osteocytes sense strain rate rather than fluid flow? BioEssays 43:2000327. https://doi.org/10.1002/bies.202000327
Spaan A (1996) *Hippopotamus creutzburgi*: The case of the Cretan Hippopotamus. In: Reese DS (ed) Pleistocene and Holocene fauna of Crete and its first settlers. Monographs in World Archaeology 28. Prehistory Press, Madison, pp 99–111.
Stewart TJ, Louys J, Miszkiewicz JJ (2021) Intra-skeletal vascular density in a bipedal hopping macropod with implications for analyses of rib histology. Anat Sci Int 96:386–99. https://doi.org/10.1007/s12565-020-00601-8
Stuenes S (1989) Taxonomy, habits, and relationships of the subfossil Madagascan hippopotami *Hippopotamus lemerlei* and *H. madagascariensis*. J Vertebr Paleontol 9:241–268. https://doi.org/10.1080/02724634.1989.10011761
Taylor LA, Rudd J, Hummel J, Clauss M, Schwitzer C (2013) Weight loss in pygmy hippos (*Choeropsis liberiensis*). In: Steck B (ed) International Studbook for the Year 2012 - Pygmy Hippopotamus. Zoo Basel, Basel, pp 20–25.
van den Hoek Ostende LW, van der Geer AAE, Wijngaarde CL (2014) Why are there no giants at the dwarf's feet? Insular micromammals in the eastern Mediterranean. In: Kostopoulos DS, Vlachos E, Tsoukala E (eds) Proceedings of the VIth International Conference on Mammoths and their Relatives, Grevena-Siatista, Greece 2014. Special Volume 102, Thessaloniki, p 209.
van der Geer A, Dermitzakis M, De Vos J (2006) Crete before the Cretans: the reign of dwarfs. Pharos 13:121–132.
van der Geer A, Lyras G, De Vos J (2021) Evolution of island mammals: adaptation and extinction of placental mammals on islands. John Wiley & Sons, Hoboken.
Von Meyer H (1832) Palaeologica zur Geschichte der Erde und ihrer Geschöpfe. Frankfurt.
Whitney MR, Otoo BK, Angielczyk KD, Pierce SE (2022) Fossil bone histology reveals ancient origins for rapid juvenile growth in tetrapods. Commun Biol 5:1280. https://doi.org/10.1038/s42003-022-04079-0
Walker MM, Louys J, Herries AI, Price GJ, Miszkiewicz JJ (2020) Humerus midshaft histology in a modern and fossil wombat. Aust Mammal 40:30–39. https://doi.org/10.1071/AM20005